V_{max} Regulation through Domain and Subunit Changes. The Active Form of Phosphoglycerate Dehydrogenase[†,‡]

James R. Thompson,[§] Jessica K. Bell,[∥] Judy Bratt,[§] Gregory A. Grant,[⊥] and Leonard J. Banaszak*[,§]

Department of Biochemistry, Molecular Biology and Biophysics, University of Minnesota, Minneapolis, Minnesota 55455, National Institute of Diabetes and Digestive and Kidney Diseases, National Institutes of Health, Bethesda, Maryland 20892, and Department of Molecular Biology and Pharmacology and Department of Medicine, Washington University, St. Louis, Missouri 63110

Received September 22, 2004; Revised Manuscript Received February 22, 2005

ABSTRACT: An active conformation of phosphoglycerate dehydrogenase (PGDH) from *Escherichia coli* has been obtained using X-ray crystallography. The X-ray crystal structure is used to examine the potential intermediates for V_{max} regulation, for the redox reaction, and for cooperative effects of serine binding. The crystal structure at 2.2 Å resolution contains bound NAD^+ cofactor, either sulfate or phosphate anions, and α-ketoglutarate, a nonphysiological substrate. A PGDH subunit is formed from three distinct domains: regulatory (RBD), substrate (SBD), and nucleotide binding (NBD). The crystal conformation of the homotetramer points to the fact that, in the absence of serine, coordinated movement of the RBD−SBD domains occurs relative to the NBD. The result is a conformational change involving the steric relationships of both the domains and the subunits. Within the active site of each subunit is a bound molecule of α-ketoglutarate and the coenzyme, NAD. The catalytic or active site cleft is changed slightly although it is still solvent exposed; therefore, the catalytic reaction probably involves additional conformational changes. By comparing the inhibited with the uninhibited complex, it is possible to describe changes in conformation that are involved in the inhibitory signal transduction of serine.

Phosphoglycerate dehydrogenase (PGDH,[1] EC 1.1.1.95) catalyzes the NAD^+-dependent oxidation of 3-phosphoglycerate into 3-phosphohydroxypyruvate, a branch point from the glycolytic pathway and the initial reaction in L-serine biosynthesis. The reaction, shown in Figure 1A, has been studied using the enzyme from *Escherichia coli* where the steady-state kinetics were found to be regulated by serine through allosteric effects on V_{max} rather than the more common K_m (*1*−*3*). In addition, the binding of serine to the tetrameric enzyme was shown to be cooperative (*4*). The catalytic reaction itself is a typical dehydrogenation involving the coenzyme NAD. Catalysis most likely proceeds through the transfer of a proton to and from a His−Glu ion pair and the movement of a hydride ion between the substrate and the coenzyme. In the L-serine metabolic pathway, the PGDH reaction shown in Figure 1A proceeds to the right and then involves a transamination. In the final step, a phosphatase removes the phosphate moiety to produce serine.

Prior crystallographic studies of PGDH in complex with serine and NAD^+ described the inhibited enzyme as a homotetramer with approximate 222-point symmetry (*5*) (PDB code 1PSD). Each subunit (44 kDa) was comprised of three domains: the serine or regulatory binding (RBD), the cofactor or nucleotide binding (NBD), and the substrate binding (SBD) domains. These background data are summarized in Figure 1B. In terms of the amino acid sequence, the domains are defined as follows: (1) NBD, residues 108−295; (2) SBD, residues 7−108 and 296−317; (3) RBD, residues 318−410. The NAD bound to the inhibited crystalline protein identified the location of the active site but provided no insight into the conformational changes accompanying serine-induced inhibition (*5*).

The quaternary structure shown in Figure 1B is unusual in that the inhibited enzyme has the shape of an ellipsoidal toroid. The overall shape of the oligomer leads to only two major subunit−subunit interfaces, between adjacent RBDs and NBDs. The inhibitor, serine, was bound between adjacent RBDs, tethering that interface. Engineered disulfide bridges between adjacent RBDs confirmed that rigidity at the RBD−RBD interface could mimic serine inhibition (*6*). Interestingly, a truncated, serine nonresponsive form of PGDH lacking the RBD remained a tetramer, suggesting that a stable third subunit−subunit interface exists in the active form of PGDH (*7*).

[†] The studies described here were funded by National Institutes of Health grants to G.A.G. (GM56671) and L.J.B. (GM13925). Use of the 19ID beamline at the Structural Biology Center at the Argonne National Laboratory was supported by the U.S. Department of Energy, Office of Energy Research, under Contract W-31-109-ENG-38. Computational time was made available by the Minnesota Supercomputing Institute.

[‡] Atomic coordinates were deposited in the Protein Data Bank (PDB; http://www.rcsb.org/pdb/; info@rcsb.org) at the Research Collaboratory for Structural Bioinformatics (RCSB; http://pdb.rutgers.edu/) with PDB code 1YBA.

* Corresponding author. E-mail: banas001@umn.edu. Phone: 612 626 6597. Fax: 612 624 5121.

[§] University of Minnesota.

[∥] National Institutes of Health.

[⊥] Washington University.

[1] Abbreviations: PGDH, D-3-phosphoglycerate dehydrogenase; Inh-PGDH, the serine inhibited form of PGDH; RBD, regulatory or serine binding domain of PGDH; NBD, NAD binding domain of PGDH; SBD, substrate binding domain of PGDH; NAD, nicotinamide adenine dinucleotide, oxidized form; CNS, Crystallographic and NMR Systems; FDH, formate dehydrogenase; AKG, α-ketoglutarate.

10.1021/bi047944b CCC: $30.25
Published on Web 03/25/2005

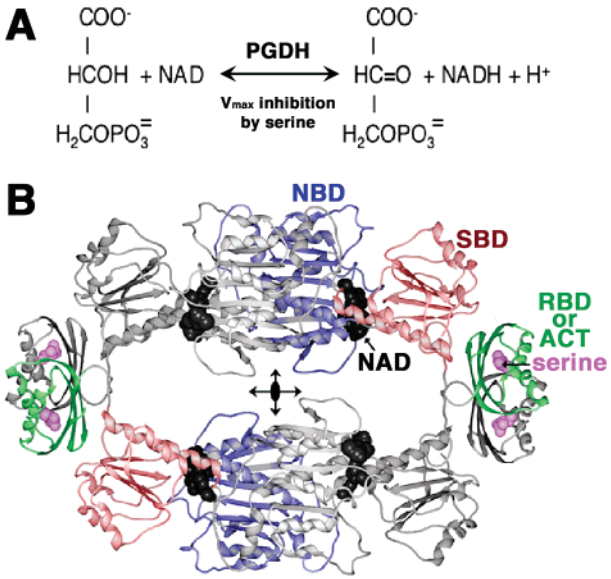

FIGURE 1: Enzymatic reaction of PGDH and its regulation. (A) The reaction catalyzed by PGDH is the first step in the biosynthesis of serine. Serine is a cooperative, V_{max}-type inhibitor of PGDH from *E. coli*. (B) The cartoon describes the crystal structure of the serine-inhibited form of PGDH. The inhibited form appears as an ellipsoidal toroid with pseudo-222-point symmetry. The arrows and ellipse in the central most part of the figure indicate the symmetry elements of the tetramer. PGDH is a three-domain structure with only two subunit interfaces in the inhibited tetramer. The two principal interfaces are those between regulatory binding domains and between nucleotide binding domains. The domains are marked in the top rightmost subunit and are labeled NBD (nucleotide binding domain, colored blue), SBD (substrate binding domain, colored red), and RBD (regulatory binding domain, colored green). The location of the serine binding sites (purple spheres) and the NADs in the active site (black sphere) indicate the separation between the allosteric/inhibitor site and the active site, respectively.

Further insight into the conformational changes necessary for catalysis and the mechanism for the allosteric inhibition arose from structurally homologous D-2-hydroxy acid dehydrogenases such as formate dehydrogenase (FDH) (*3*, *8*). PGDH differs from other D-2-hydroxy acid dehydrogenases in that it is a tetramer rather than a dimer and has the C-terminal RBD. Otherwise, the structural similarities between the SBD and NBD of these family members allowed parallels to be drawn on potential conformational changes occurring during catalysis. In FDH, the relative change in orientation of the two component domains (SBD and NBD) was found to be dependent on the presence of bound substrate and cofactor. The domain reorientation, an approximate 7° rotation of the SBD toward the NBD, was necessary for a productive catalytic cycle (*8*). In the context of the PGDH tetramer, a similar change in domain−domain orientation was proposed to be related to the serine control mechanism of PGDH (*9*).

The polypeptide segments necessary for domain reorientation have been identified by both structural and biochemical analysis. The crystal structure of a PGDH mutant (W139G, PDB code 1SC6) when compared to the inhibited enzyme delineated two such sites: (1) F102−F106 and (2) T297−Q298 (*10*). Grant et al. also observed that when two Gly-Gly sequences (residues G294−G295 and G336−G337) between the NBD−SBD and SBD−RBD were mutated to valine, catalysis and the ability of serine to inhibit catalysis were reduced (*11*). Taken together, these experiments identified flexible regions and their potential effects on catalysis but not the conformational changes necessary for allosteric control that are propagated from the serine binding site in the RBD to the active site.

The RBD domains of PGDH are comprised of approximately 100 amino acids. The conformation at the RBD−RBD interface is formed by the linkage of three β-strands from each subunit forming a six-stranded β-sheet across the interface. In the inhibited structure, the serine binding sites occur in a manner that results in interactions with both subunits across the interface at the end regions of the continuous β-sheet (*5*). Because of the symmetry of the tetramer, two identical serine sites are located relatively close to each other.

Amino acid sequence homology shows that RBD-like domains are contained in other enzymes in amino acid and purine metabolism (*12*, *13*). Like PGDH, the homology appears to be present in these enzymes at the COOH termini, and the conformation has now been labeled the ACT domain (*12*).

In the accompanying Results section, the similarities and differences between the active and inhibited forms of PGDH are described. The ubiquitous presence of RBDs in enzymes elevates the need to understand the mechanism of both the allosteric inhibition by serine and the cooperativity of serine binding in PGDH. Aided by the homology of PGDH to other D-2-hydroxy acid dehydrogenases, new insights into the mechanism of allosteric control via the RBD or ACT domains are developed and described below.

MATERIALS AND METHODS

All chemicals were purchased from Sigma-Aldrich and were of research grade unless specifically indicated otherwise. 5′-AMP−Sepharose was obtained from Pharmacia. Protein concentration was determined conventionally by absorbance at 280 nm using an $E^{1\%} = 6.7$ and after purification by the Bradford method. The enzyme was assayed for activity at a constant 25 °C in 20 mM Tris buffer at pH 7.5 by monitoring a decrease in absorbance of NADH at 340 nm with either α-ketoglutarate or 3-phosphohydroxypyruvate as a substrate (*14*, *15*).

Purification and Crystallization of Se-Met PGDH. The plasmid used for protein production has been described earlier (*7*, *16*). Selenomethionine-substituted PGDH was prepared using *E. coli* B834(DE3), a methionine-requiring auxotroph (*17*, *18*). Induction with 1.5 mM isopropyl thiogalactoside was carried out following a 37 °C growth period to an OD_{600nm} of 1.0. Four hours after induction, cells were harvested and frozen for later use.

At the start of purification, the cell pellet was resuspended into 50 mM potassium phosphate buffer, pH 7.0, containing 2 mM DTT, 1 mM EDTA, and 0.05% NaN_3 (buffer A), and the cells were lysed by pulses of sonication with the sample in an ice bath. The initial cell lysate was clarified by centrifugation at 10000*g* for 30 min, and the PGDH within the supernatant was then purified as published previously (*16*). A comparison of the electrospray mass spectra of this Se-Met sample to that of native PGDH indicated that eight selenium sites were incorporated per PGDH monomer. After confirming the Se-Met protein had wild-type activity, pure recombinant PGDH was concentrated to 12 mg/mL and

Table 1: X-ray Data for Serine-Free PGDH

unit cell (Å; deg)	$a, b = 73.48$, $c = 354.02$; $\alpha, \beta, \gamma = 90$		
space group	$P4_3$		
data set (Å)	remote 0.9537	inflection 0.9795	peak 0.9797
resolution range (Å)	50.00−2.24	50.00−2.24	50.00−2.24
outer shell	2.28−2.24	2.28−2.24	2.28−2.24
unique reflections	93815	91720	92508
outer shell	3786	3201	3598
completeness (%)	97.5	95.2	96.3
outer shell	79.9	67.4	77.3
redundancy	12.1	11.7	12.2
outer shell	2.0	1.9	2.1
$\langle I \rangle / \sigma I$	21.8	22.3	20.2
outer shell	2.3	2.3	2.3
R_{merge}[a] (%)	8.3	8.0	8.9
outer shell	45	41	45
f'	−4.1	−7.6	−10.7
f''	3.6	6.6	3.1

[a] R_{merge} shown $= (\sum |I - \langle I \rangle| / \sum I) \times 100$.

exchanged into a fresh solution of buffer A with a Centriprep 10K (Amicon).

The conditions used to obtain the Se-Met PGDH crystals for MAD and the unit cell parameters were similar to those reported earlier (*16*). Just prior to crystallization, fresh NAD^+ and α-ketoglutarate were added to the protein stock to concentrations of 2 and 5 mM, respectively. Three microliters of this modified stock was mixed with 3 μL of the precipitant from the well of a 24-well Linbro plate. Equilibration was carried out at 18 °C. Precipitant wells resulting in crystals varied from 1.18 to 1.25 M ammonium sulfate and 100 mM potassium phosphate with an optimal pH of 6.4. Rod-shaped crystals up to $0.2 \times 0.2 \times 0.8$ mm^3 grew over the range of 1 h to 2 weeks. Cryoprotection was done by the slow addition of solid xylitol directly into the edge of a droplet of mother liquor until the X-ray ice rings were absent from the mother liquor at 100 K. The same droplet contained the enzyme crystals.

Crystallographic Methods. X-ray diffraction data were collected from vetted crystals on beamline 19ID of the Structural Biology Center at the Advanced Photon Source (Argonne National Laboratory, Argonne, IL). Prior MAD experiments on Se-Met PGDH crystals elsewhere revealed that the small beam focus of 19ID was ideally suited to the long *c*-axis length of the unit cell. Also, key to high quality diffraction data was the placement of the APS1 CCD area detector at a distance of 400 mm to minimize overlaps. Crystals were oriented so that the *c*-axis was roughly 10° off parallel to the spindle axis of the goniometer prior to data collection. A gaseous nitrogen cryostat from Oxford Cryosystems was used to maintain a temperature of 100 K.

For one crystal of $0.08 \times 0.11 \times 0.23$ mm^3, a scan of X-ray fluorescence indicated a strong and homogeneous selenium signal. On the basis of this scan, we recorded three unique data sets at the peak, inflection, and a low energy remote of the fluorescence spectrum (see Table 1). The selenium atom substructure was easily located by the program SOLVE (version 2.03) (*19*) using all three wavelengths with the measured dispersive and anomalous differences up to a resolution of 2.24 Å.

Refinement of the initial, full tetramer against the remote wavelength data was carried out using torsion angle molecular dynamics and the phase-restrained MLHL target as implemented in CNS (*20*). All diffraction data from 50 to 2.24 Å were applied throughout the refinement but for 4538 randomly selected reflections for cross-validation of the maximum likelihood target and R_{free} calculations. Maps of electron density were calculated with CNS using phases calculated from the MLHL refined model combined with the MAD experimental phases. Twelve iterative cycles of model rebuilding, positional refinement, restrained *B*-factor refinement, and water placement ensued. NCS restraints were used initially during refinement but were relaxed after the first cycle. Likewise, side-chain rotamers that were NCS-related were at first made equivalent. Solvent molecules were identified when spherical $2F_o - F_c$ and $F_o - F_c$ electron density was observed at 1σ and 3σ, respectively. Solvent finding and evaluating algorithms within CNS and WARP were also used (*21*). Default parameters for the required electron density threshold and the distance between hetero-atom atoms were employed.

Table 2: Phasing and Refinement Statistics for Crystalline PGDH

Z-score (SOLVE)	157
FOM (MAD/density mod)	0.51/0.58
resolution range (Å)	50.0−2.24
R_{factor}/R_{free} (%)	18.6/23.5
estd coordinate error based on R_{free} (Å)	0.22
no. of atoms	
protein	12360
ligand	311
water	1346
RMS deviation from ideality	
bonds (Å)	0.018
angles (deg)	1.69
average *B*-factors (Å^2)	
main chain	18.2
side chain	22.6
ligands	37.2
solvent	37.6

Domains and domain−domain conformational changes were located visually or by using the method and computer program DYNDOM devised by Hayward and co-workers (*22*, *23*). The figures in this report were made with either SPOCK (*29*) or PYMOL (*24*).

RESULTS

Details of the X-ray diffraction data are summarized in Table 1. Data to 2 Å were observed and collected, but on later analysis the maximum resolution was assigned as 2.24 Å for each wavelength because of the low signal to noise ratio. After selenium positions were refined, experimental phases were obtained from the anomalous differences of the 32 Se sites in the asymmetric unit. The FOM was 0.51 for the MAD phases between 50 and 2.24 Å resolution. The averaged electron density computed by RESOLVE was sufficiently good that the entire tetramer of PGDH was completed prior to the use of any model refinement. An anomalous difference Fourier map confirmed the placement of all expected selenium sites, and a summary of the coordinate data after refinement and model building is presented in Table 2.

In addition to phase enhancement by solvent flattening, RESOLVE was able to determine the location of operators for noncrystallographic symmetry present in select regions of the asymmetric unit, and averaging of these smaller

volumes was used to improve the MAD phases. These modified phases resulted in a FOM of 0.58 to a resolution of 2.24 Å. Automated chain tracing was carried out in RESOLVE, providing an initial model for 78% of the overall structure (*19*). Only a few errors in the automatic tracing needed correction using the program O (*30*). The finished structure of the four subunits of serine-free PGDH per asymmetric unit has a correlation coefficient (F_o versus F_c) of 94% and an estimated coordinate error of 0.24 Å (based on R_{free}). The $F_o - F_c$ difference map is comparatively flat, with a standard deviation of 0.51 e/Å^3 before normalization.

The final model of the PGDH tetramer consists of 12360 protein atoms and 311 heteroatoms. In the latter group are one α-ketoglutarate and an NAD^+ molecule at the active site of each subunit. There are also four anions of either PO_4^{3-} or SO_4^{2-} per tetramer. Last of all, there is an unknown molecule attached to each PGDH subunit near the outer limits of the active site cleft. From the shape of its electron density, it appears to be another AKG molecule. However, the identifying designation UNK is used in the coordinate list to differentiate the externally bound molecules from those AKGs at the active sites. Lastly, there were 1346 sites that obey the accepted criteria for water molecules and are included in the crystallographic coordinates. The summary of atom components as used in the refinement is given in Table 2 along with the average *B*-factors for protein, ligands, and solvent atoms.

The stereochemical quality of the protein model was analyzed with PROCHECK (*25*) and by the WHATCHECK server (*31*). The model has 99.6% of the main-chain torsional angles within the allowed and expanded regions of the Ramachandran plot. No side chains have disallowed ϕ,ψ angles. The coordinates of the PGDH structure have been deposited in the Protein Data Bank, with the identification code 1YBA. When combined with the information from the crystal structures of Inh-PGDH and the mutant form, W139G-PGDH, it is now possible to analyze the different structural states in terms of the conformational changes, which must occur during the allosteric inhibition by serine.

Quaternary Structure of Active PGDH. The crystal structure of active PGDH from *E. coli* exists as a homotetramer with some visible changes compared to the quaternary structure of the serine-inhibited enzyme. To compare the two conformations, surface representations are shown side by side in Figure 2A, and the two different tetramers are oriented such that two dyads are within the plane of the drawing. The domains are labeled in the model of the active form, and the subunits of the tetramer are shaded the same way for both forms of the enzyme and are labeled A through D.

The subunit−subunit interactions may be compared as follows. In the serine-inhibited PGDH, the contacts are between A and D or between B and C through the RBDs or ACT domains and between A and B or between C and D through the NBD domains. The same subunit contacts between RBDs and NBDs are preserved in the active form. However, new intersubunit contacts are formed nearest the 2-fold rotation axis perpendicular to the drawing and are indicated by an oval at the center of Figure 2A. The novel interactions are not extensive but occur from subunits A to C and from subunits B to D now through the NBD domains. The new subunit−subunit contacts are mainly mediated through bound solvent molecules. The region marked by the 2-fold axis perpendicular to the drawing in Figure 2A is shown in greater detail in Figure 2B with the new contacts between the NBDs of subunits A and C at the left and the NBDs of subunits B and D at the right. Hydrogen bonds are marked if shorter than 3.8 Å. The prime residues involved are N190 and Y176, and also R150 in one case.

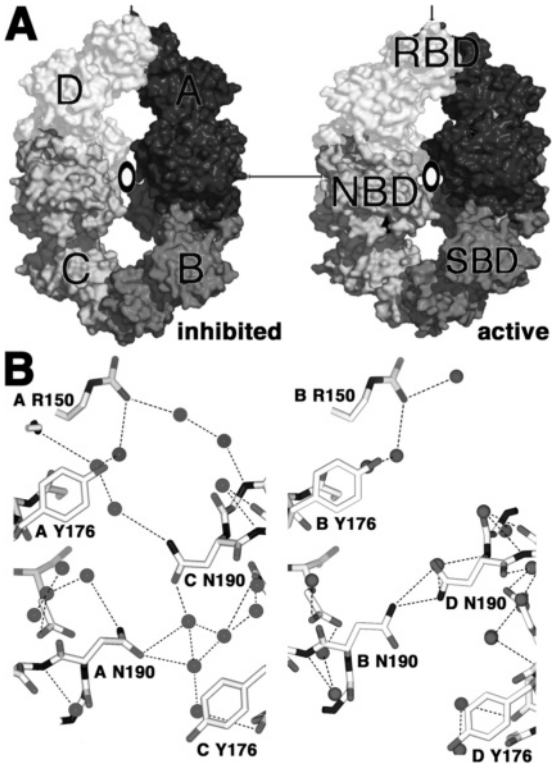

FIGURE 2: Quaternary conformation of serine-inhibited and active PGDH. (A) Using the crystallographic coordinates described in the text, a surface representation of the serine-inhibited (leftmost drawing) and active form of PGDH is shown. Conformational states are labeled to aid the reader in observing the important quaternary and tertiary structural changes. In the inhibited form (leftmost), each subunit is labeled as A, B, C, and D and shaded uniquely. In the active form of PGDH (rightmost) the same shading is present but the abbreviations RBD, NBD, and SBD are present to indicate the approximate locations of the domains mentioned in the text. The black lines and ellipse denote the presence of the symmetry elements of the tetramer. Note the additional contacts formed between A and C and between B and D in the active form of the enzyme. (B) In the active PGDH, hydrogen bond interactions are found between the NBD domains of the A and C (left) and the B and D (right) subunits. The novel interface as observed is mainly mediated by bound water molecules with the exception of a single hydrogen bond between the side chains of N190. All hydrogen bonds were calculated with HBPLUS with a 3.8 Å distance cutoff.

To summarize, there are clearly some quaternary changes between the serine-inhibited and the active forms of crystalline PGDH. In the transition toward the active enzyme, some additional subunit−subunit contacts are made around the 2-fold axis that had the weakest interactions in the inhibited enzyme. To analyze these conformational changes, three steps were undertaken: (1) the overall domain−domain reorientation was analyzed, (2) next, changes in the RBD depending on the presence of bound serine were evaluated, and (3) finally, changes at the active site were probed on the basis of the two chain segments linking an SBD and to an NBD domain.

Conformational Changes through Domain−Domain Reorientation in PGDH. When two conformational states of a

multidomain, multisubunit protein are to be compared, the selection of a subset of the coordinates to represent a reference or fixed segment is ambiguous. For the transition of the PGDH tetramer from the totally inhibited conformation to the uninhibited state, the following observations were made. Only minor quaternary changes occur at the RBD−RBD and NBD−NBD subunit interfaces. Furthermore, the conformation of the combined RBD−SBD segments of a single subunit was shown to be unaffected. Finally, the NBD domains are superimposable in both the inhibited and active states. With these observations in mind, the comparison of the two allosteric states of PGDH is summarized as follows.

When a least squares superposition is computed using the C_α coordinates of residues 7−410 (all possible) for all four subunits (not shown), the main conformational differences occur between domains with few changes at subunit−subunit interfaces. For example, there are no major conformational differences suggestive of a "piano hinge" at the RBD−RBD interface where the three β-strands from each subunit interact to form a six-membered sheet (*6*). Instead, the conformational comparisons suggest that each subunit's RBD and SBD, and the RBD and SBD domains of the monomer related by a RBD−RBD interface, move as a rigid body (see Figure 2). Similarly, the NBDs of subunits A and B in Figure 2 (and subunits C and D) also appear to act as rigid bodies. This is not surprising given the extensive interface with an interaction area of over 2000 Å^2 at the NBD−NBD junction.

Although visible changes were observed in the quaternary structure of PGDH compared to Inh-PGDH, the key conformational differences were visible when the X-ray coordinates were compared within a single subunit of the active and inhibited enzymes. These domain−domain changes were first analyzed by DYNDOM, a numerical method developed by Hayward and co-workers (*22*, *26*). The algorithm is a form of normal-mode analysis that provides unique nonsubjective descriptions of domains and, for two interrelated structures, the screw operation for their stereochemical correlation (*22*). To do this, DYNDOM calculates unit vectors to all atoms and then determines the formation of clusters. For conformational changes of PGDH, the domain analyses were particularly informative since they could be compared with even larger differences observed in the crystal structure of W139G-PGDH (*10*).

However, the conformational comparisons are complicated by the 222-point symmetry of the tetramers. For PGDH, the asymmetric unit contains a tetramer, and the local dyads relating monomers are not exact. The RMSD values of the C_α positions among all possible pairing of subunits are given in Table 3. The polypeptide subunits across the NBD−NBD interface (A to B in Figure 2A) are more exactly superimposable than the monomers sharing a RBD−RBD interface (A to D). With respect to the differences observed in the crystal lattice of the uninhibited PGDH, the D monomer shown in Figure 2A appears to contain the largest coordinate disparity. Two loop segments are responsible for the noted differences; one involves the conformation around G362, and the other is a loop involving the amino acid sequence segment from N184 to S216.

The crystals of Inh-PGDH contained a dimer in the asymmetric unit, and so one of the dyads was crystallographic (*5*). In the Inh-PGDH structure, the RBD−RBD interface is related by crystallographic symmetry whereas the local dyad symmetry is at the NBD−NBD junction. Since the conformational differences between the two forms of PGDH are the prime reason for the X-ray study, additional internal comparisons were made of the coordinates of the active subunits as well as gross comparisons to the serine-inhibited enzyme in Table 3.

Table 3: RMSD[a] between Serine-Free and Inhibited PGDH Monomers

	Se-Met B (Å)	Se-Met C (Å)	Se-Met D (Å)	serine A (Å)	serine B (Å)
Se-Met A	0.52	0.84	1.24	2.04	1.11
Se-Met B		0.76	1.04	1.88	0.94
Se-Met C			0.96	1.78	0.72
Se-Met D				1.55	0.98
serine A					1.46

[a] RMSD is the root mean square distance difference between C_αs of overlaid coordinates determined independently in the crystal structure. Se-Met A−D refer to uninhibited PGDH subunits. Serine A and B refer to inhibited PGDH subunits.

Table 4: Domain−Domain Changes in Crystal Structures of PGDH

(A) conformer	fixed domain	moving domain	T_{angle} (deg)	T (Å)
native vs inhibited	11−106, 299−408	107−298 (NBD)	15	−0.5
native vs W139G[a]	9−102, 297−408	103−296	27	−0.7

(B) hinge	bend residues
native vs inhibited	104−107, 298−299
native vs W139G[a]	102−103, 291−301

[a] Reference *10*.

A comparison of subunit A in the inhibited and uninhibited states is shown in stereo in Figure 3. As noted earlier, the structural relationship between the RBD and SBD in the two states of the enzyme is unchanged. Hence the changes following serine binding may be primarily described as the reorientation of the NBD relative to an RBD−SBD unit along with the accompanying subunit rearrangement of the tetramer. The black arrow in Figure 3 marks a screw transformation that describes the conformational change consisting of an angular rotation of 15° and a translation of 0.5 Å. Note however, that the translational change is close to the experimental error in the coordinates and may essentially be ignored. The same operator is shown in Figures 4 and 5 to serve as a reference guide to the conformational change as different segments of a subunit are depicted.

The linkages between an RBD−SBD unit and the NBD are also labeled with the caption "hinges". There are two segments of polypeptide that link the SBD to the NBD. Upon serine binding, it is at this double crossover that conformational changes must occur to produce changes in the catalytic activity. The domain−domain reconfiguration described in Figure 3 occurs through residues 104−107 and 293−297. These two connecting segments must be central to the allosteric effect. Their role in the domain−domain changes is supported by the fact that they are also involved in the reorientations found in the crystal structure of mutant PGDH, W139G (*10*).

To summarize these observations: the conformational changes occurring during serine inhibition are characterized by bending about the same region of the PGDH subunit as had been observed with W139G-PGDH. The screw motion

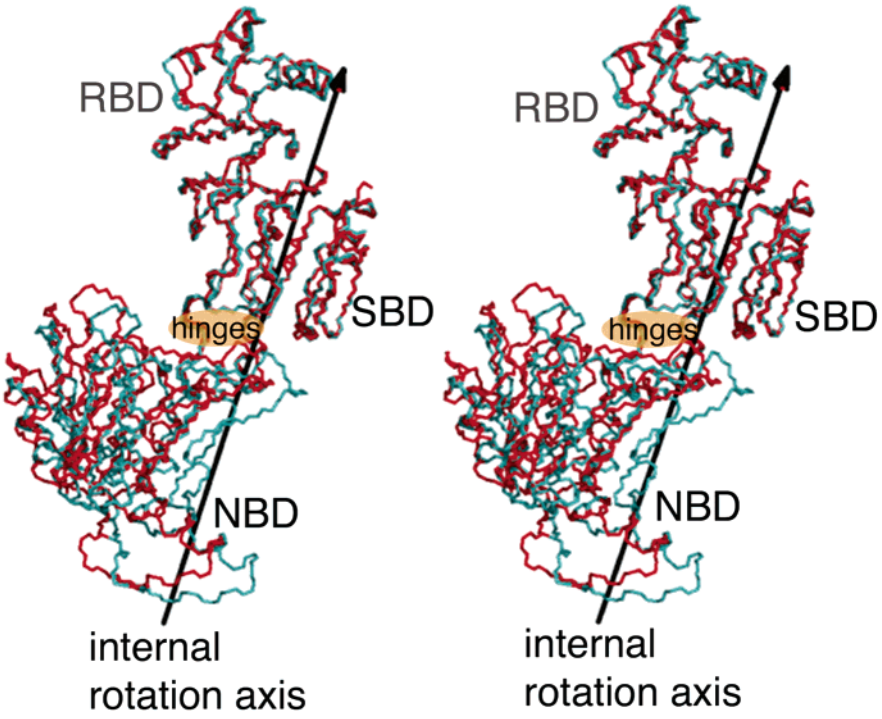

FIGURE 3: Conformational changes in PGDH resulting from binding in the regulatory domain. The image contains the C_α models of subunit A from the crystal structures of PGDH (blue) and Inh-PGDH (red). The three domains (NBD, SBD, and RBD or ACT) are labeled as in Figure 2. In this representation, the RBD and SBD from both crystal structures are essentially superimposable with the conformational change represented by the movement of NBDs. The arrow describes the rotation/translation for the allosteric transition.

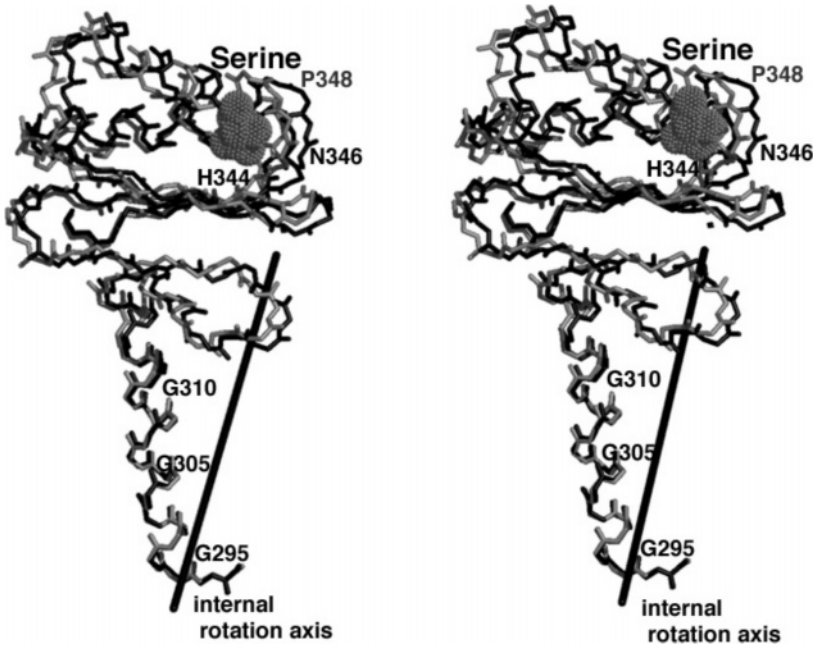

FIGURE 4: Signaling by serine. The stereo diagram contains an overlay of the X-ray coordinates of active (black) and serine-inhibited forms (gray) of an RBD domain from the crystal structures of PGDH (subunit A). The bound serine molecule in the inhibited form is shown as gray balls. A few labels in the RBD mark the position of residues discussed more fully in the text. The position of the transformation operator as determined by DYNDOM is depicted as a black line. The conformational differences apparent in the drawing appear after the least squares superpositioning of the helix between G_{295} and Y_{315}. Using this helical segment as a template, the conformational changes in the RBD as a result of serine binding become more apparent. The major conformational difference is the relatively large movement occurring at P348.

in both cases involves essentially no translational component, and the parts of the subunit that change relative orientation are the same: RBD−SBD 11−106 and 299−408 and NBD 107−298. The rotation relating the native to the serine inhibited is 15°; that relating the native to the mutant W139G is 27°. There was also good agreement defining the hinge residues: (1) Nat vs serine inhibited involved residues 104−107 and 298−299. (2) For Nat vs W139G the bend residues were 102−103 and 291−301.

Signaling by Serine at the RBD Domain. The initiation of serine signaling begins with the binding of serine molecules at the interface between RBDs (see Figure 1). Having located

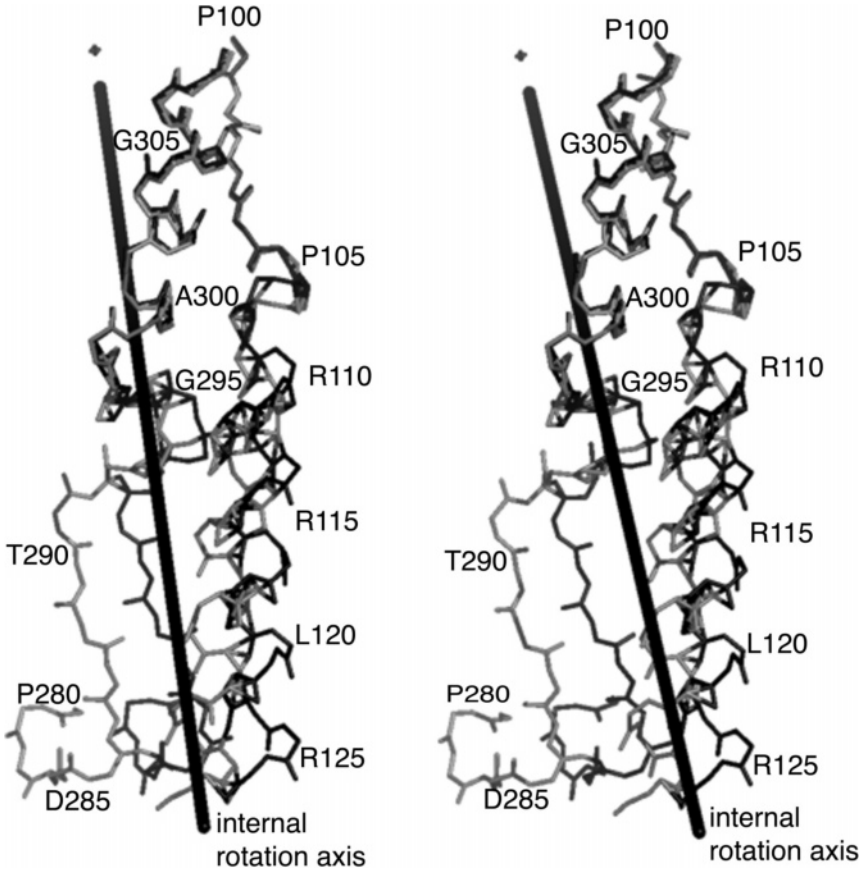

FIGURE 5: The subunit conformational change is transmitted through the crossovers to the NBD. The NBD domain of PGDH is connected to the remainder of the molecule (SBD−RBD) by two segments of polypeptide chain. This region as shown in this cross-eye stereoview includes residues P100−V112 and I293−V308. The amino acid sequences through the two linker regions are P_{100}VFNAPFSNTRSV-AELVIGELLLR_{125} and P_{280}LCEFDNVLLTPHQIGGSTQEAQENIGLEVG$_{310}$. I293 is immediately adjacent to the catalytic histidine H294, so an observed peptide flip at this position is of interest to the catalytic mechanism. The stereo image is an overlay of the crystal coordinates from the serine-inhibited enzyme (gray bonds) and the active form (black carbon bonds). The heavy black line marks the position of the transformation axis for the conformational change occurring during the V_{max} allosteric change in the presence of serine as determined by DYNDOM (see accompanying text).

the hinge necessary for the reorientation of the NBD relative to the SBD−RBD, similar comparisons of the X-ray coordinates were used to search for the differences in the RBD that drive the conformational changes at these crossovers. To make the necessary conformational comparisons, the inhibited and active coordinates of RBD−SBD were overlaid by least squares methods using the main-chain atoms of residues 295−310. The RMSDs for this segment were 0.43 Å for all backbone atoms and 0.96 Å for all atoms. The overlaid RBD domains are shown in Figure 4. The active form of PGDH is displayed in black, the inhibited structure is in gray, and the bound serine is visible as the dotted surface. The polypeptide segment from 295 to 310 is an α-helix running from the RBD down the side of the SBD to the crossover with an NBD.

A major conformational difference is visible at the top of Figure 4 centered on P348; the variation involves a loop positioned over the serine binding site. This loop has the amino acid sequence -H_{344}-E-N-R-P-G_{349}-.

In the serine binding site, NE2 of H344 is hydrogen bonded to both oxygens of the serine effector in what appears to be a tight salt bridge (*5*). In addition, the nitrogen atom of the bound serine forms a hydrogen bond with the side chain of N346. The bound inhibitor spans the RBD−RBD interface forming a hydrogen bond with a second asparagine, N364′ of the adjacent subunit (*5*), such that these interactions and any subsequent conformational changes confer both the subunit inhibition and intersubunit cooperativity.

In the serine-bound form of PGDH, the N346−serine- - - N364′ network provides an additional hydrogen bond across the RBD interface at each effector site. In the new position of the P348 loop closed over the inhibitor, several new interactions are formed. The main-chain carbonyl oxygen of G349 forms a hydrogen bond with the main-chain nitrogen of A353. The side-chain carboxyl of E384 is also in position to hydrogen bond to the amide nitrogen of N364′, the main-chain carbonyl oxygen of Q375 interacts with the main-chain nitrogen of N346, and the guanidino nitrogen of R347 hydrogen bonds to the main-chain carboxyl of P401. Whereas the binding of serine results in direct hydrogen bonds and salt bridges to the ligand and a slight shift at the interface, this slight shift results in a lengthening or breaking of the main-chain hydrogen bond between the carbonyl oxygens of T372 and A366 present in the native structure.

The maximum magnitude of these conformational differences between the inhibited and active forms around the inhibitor molecule is represented by the CG atom of P348, which moves about 4 Å upon inhibitor binding. It is important to note that this distance is very much dependent on the atoms used to specify the transformation between conformations. As now ascertained from the uninhibited

crystal structure, a series of small conformational changes and a few new noncovalent interactions result from inhibitor binding.

The residues immediately below the serine molecule forming the inter-RBD β-sheet superimpose very well across adjacent subunits. This supports a previous observation that the intersubunit β-sheet (SBD to SBD) does not appear to undergo a conformational change during domain reorientation (*10*). Since the distance between the allosteric and active site is large, 35−40 Å, the many alterations that communicate changes upon serine binding down to the active site are still masked. Even so, the rotation around the "internal rotation axis" as indicated in Figure 4 explains the changes in the NBD to RBD−SBD domain arrangement.

The RBD−SBD to NBD Linker Region in PGDH. As note above, the movement of the RBD−SBD region relative to the NBD domain may be described by a rotational motion at the polypeptide segments that link them together. In PGDH, any domain−domain conformational change is complicated by the fact that the interconnecting polypeptide chain between the RBD−SBD and NBD includes a double crossover. The two crossovers connecting the NBD and SBD are relatively close to each other in the overall structure. This can be seen in Figure 5 where the polypeptide segments of the crossover are shown. In particular, S107 to R110 and G294 to Q301 visibly cross a gap between each RBD−SBD and the NBD domains. Each gap contains one catalytic cleft. Thus, an important point is that linker regions appear to be positioned to affect the opening and closing of an active site cleft and, therefore, catalysis.

By means of the image shown in Figure 5 and a careful examination of the changes in ϕ,ψ angles throughout these crossover segments, the conformational changes are identifiable. The appearance of the overlay of the active (black carbon atoms) and inhibited (gray carbons) PGDHs depends on the residues used to minimize the atom-to-atom separation. Figure 5 uses a superposition determined by the DYNDOM program, a fit of the A subunits that includes 203 residues (amino acids 11−61, 64−106, 299−407), basically all of the SBD and RBD domains with a resulting RMSD of 0.71 Å.

One method of identifying important hinge residues is the comparison of ϕ,ψ angles: large deviations between two related structures are indicative of conformationally altered residues. In the P100−R125 crossover, immediately C-terminal from the SBD, structural changes occurring through ϕ,ψ changes in P105, ϕ changes in F106, and ϕ,ψ changes in N108 are all visible. The side chain of N108 is likely to interact with substrate molecules when bound within an active site. The ϕ,ψ changes are on the order of 30° where the standard deviation or σ values for ϕ,ψ obtained by examining the multiple copies of subunits was 9°.

The second strand of the crossover region is to the left in Figure 5 and includes residues P280−P310. This conformational change appears to be a product of a ψ change of 181° for I293 (peptide flip), followed by ϕ alteration for G294, and a ψ change for G295. Significant modifications also occur in S296 (ϕ) and T297 (ψ). Beyond any effect on the closure of the active site crevasse, a peptide flip at I293 probably affects the proper positioning of the catalytic histidine, H292. H292 is believed to serve as a base removing a proton from the −OH group of the substrate when the catalytic reaction is in the direction of the serine production. G294 and G295 appear to be important for defining the NAD binding site. Overall, this -G-G- sequence must permit a degree of flexibility in this portion of the double crossover.

The two-stranded domain crossover contains five hydrogen bonds that are unique to one or the other structure. With a rotamer change, the side chain of T297 in Inh-PGDH becomes hydrogen bonded to S111 on the other strand of the domain link. The T109 side chain also forms a hydrogen bond with the carbonyl of F106. A change of the rotamer of N303 allows two hydrogen bonds in the active PGDH to the carbonyl atoms of S107 and A300. Finally, the carbonyl of G294 bonds to the main-chain nitrogen of V122. The latter bond appears to maintain the peptide carbonyl flip seen for the neighboring I293. These noncovalent bonds, present in all subunits, may impart important communication between the two strands of the domain crossovers and act to stabilize appropriate main-chain conformations.

In the previous section, serine binding led to conformational changes in a loop region of the RBD causing changes in the ϕ,ψ angles of several residues in the crossover region between the SBD and NBD. Taken together, the allosteric change involves the rotation of an NBD relative to the corresponding RBD−SBD domains.

The Active Site. The conformation of PGDH in the absence of serine provided an image of the active site in an abortive ternary complex containing NAD and AKG (α-ketoglutarate). The crystallographic results pertaining to the active site are summarized in Figure 6. The extent of the crystal structure described in Figure 6 has been increased due to the presence of multiple AKG molecules bound to the crystalline enzyme.

PGDH is an A-side specific dehydrogenase. For this type of dehydrogenase, the glycosidic bond to the nicotinamide ring of the bound NAD is generally in the anti conformation, and this is the case in the present crystal structure described in Figure 6. The AKG is oriented nearly correctly but not in the optimal position for the two elements of the catalytic reaction to take place: the transfer of a proton and a hydride ion from H292 and NADH, respectively. The molecule of AKG appears to have its α-carboxylate moiety interacting with the side chains of R60, R62, and K141. The carbonyl group of AKG is a little over 5 Å from the histidine−glutamic acid pair that is likely to be the initial acceptor for the proton. The C4 atom of the nicotinamide ring is nearly 8 Å from the substrate carbonyl. Ideally, the carboxyl of AKG would be anchored by R240 to position the substrate nearer the nicotinamide for productive turnover.

The crystal structure of the uninhibited nonproductive ternary complex confirms the original proposed active site participants (*27*). R60 and R62, which are contained in the SBD, and K141′, which is contributed by the adjacent subunit, appear to interact with the substrate. The crystal structure described here is poised for the catalytic process to occur, but additional minor conformational changes must precede the final steps in the reaction. Given the distance between substrate and cofactor in order to complete a catalytic cycle, the active site cleft must close further. As in FDH (*8*), this closing most likely takes place by additional rotation about the hinge described above and a greater number of contacts within the newly defined NBD interfaces shown in Figure 2B. Further closure of the active site cleft

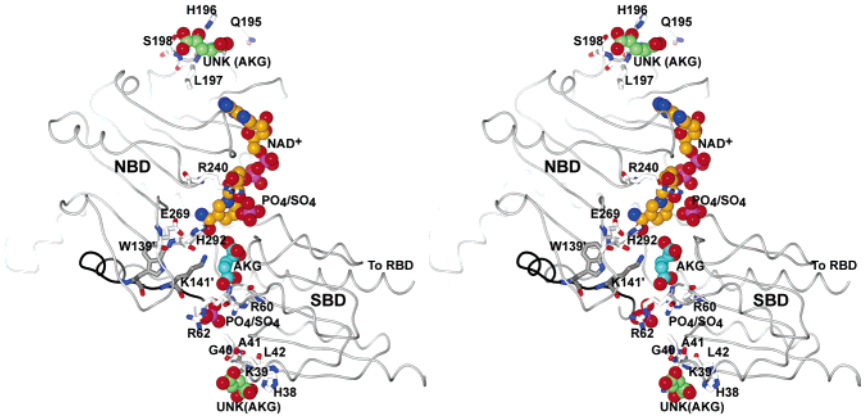

FIGURE 6: The active site of PGDH in the absence of serine. A cross-eye stereoview shows the catalytic site of subunit A. Residues implicated in catalysis (H292, E269, R240, R62, R60, K141′) or bound to ligands (H38, K39, G40, A41, L42, Q195, H196, L197, S198) are labeled. Residues from the adjacent subunit are indicated with a prime following the residue number and have gray C_αs and a black backbone. Each of the ligands is also identified. Both molecules modeled as α-ketoglutarate found outside the catalytic cavity (top and bottom with carbon atoms in violet) are shown as UNK due to the poorer quality of the electron density supporting their presence. Much better density exists for the AKG within the catalytic cleft shown with cyan carbon atoms. Notice that this substrate is correctly oriented but is not yet close enough to H292 or the nicotinamide ring for catalysis. The same situation is found within each of the four subunits in the serine-free PGDH. The NAD^+ structure, yellow C_αs, remains unchanged from that in the inhibited PGDH. The PO_4 or SO_4 anions have not been observed in a PGDH structure previously.

would serve to bring the substrate in position to react with H292 and NADH, which are contained in the NBD. The current structure contains PO_4 or SO_4 ions from the crystallization conditions that seem to compete with the substrate for hydrogen bonds to R240. We postulate that, in the absence of PO_4/SO_4 ions, the interaction between R240 and the carboxyl of the substrate would initiate cleft closure for catalysis. The other molecules modeled as AKG that also appear bound to the crystalline protein, but at the far open edge of the active site, are of unknown significance.

DISCUSSION

Phosphoglycerate dehydrogenase, a branch point to serine biosynthesis from the glycolytic pathway, is regulated by serine. Other workers have suggested that the segment that binds serine is a common fold named the ACT domains. As such, the structural studies described in this report may offer insightful background for the control mechanisms of many enzymes (*12*, *13*) and should be an important addition to signal transduction mechanisms.

Prior to this study, a description of the mechanistic intermediates of PGDH control lacked structural information on the active form of the enzyme. By comparisons of active and inactive crystal structures, the V_{max} regulation of PGDH from *E. coli* is now shown to involve a tertiary conformational change accompanied by domain−domain and subunit reorientation. The assignment of the binding activity of the domains as regulatory binding or serine binding domain (RBD), substrate binding domain (SBD), and NAD binding domain (NBD) has proven to be the case as established by the positioning of AKG in the active site of the uninhibited PGDH.

Using different sets of atoms to produce a variety of molecular overlays, it has been possible to trace many of the conformational changes that have occurred during the serine inhibition. Several conformational changes are needed to understand the intermediates in the control mechanism. The important features are summarized as follows: (1) Originally, we proposed that the three domains comprising a single subunit might be reoriented independently. This does not appear to be the case; the RBD and SBD appear to behave as a single unit, and many of the conformational differences may be described by a rotation and a small, negligible translation between the RBD/SBD unit and the NBD. The rotation is about an arbitrary axis located near to the polypeptide segments that connect the RBD−SBD to the NBD, a location referred to as "the crossover" above. (2) The active site occurs between the RBD−SBD and NBD in a cleft that is highly homologous with dimeric proteins lacking the RBDs (*8*). In fact, the RBD domains may be removed from PGDH leaving a catalytically active chimeric enzyme (*7*). Changes in the cleft opening are predicted to be necessary to complete a catalytic reaction, as is the case for the dimeric homologues. (3) The toroidal arrangement of subunits in PGDH is capable of a number of subunit rearrangements, not all of which are directly related to the allosteric control mechanism (*10*). The PGDH tetramer has the common 222-point symmetry but has only two strong subunit−subunit contacts: between two RBDs and between two NBDs. This is a somewhat unusual arrangement since homotetramers tend to have contacts across all three symmetry dyads.

The triggering chemical reaction for the allosteric inhibition and transition is the binding of the first molecule of serine. This is a positively cooperative process for the second molecule and under some conditions negatively cooperative for subsequent ligands (*28*). In terms of an RBD−RBD subunit interface, early work demonstrated that the serine had noncovalent interactions with atoms from two subunits but the binding sites were still well separated (*5*). A detailed comparison of the conformation of RBDs from the serine-inhibited and abortive enzyme had an observable conformational difference. The change consisted of the movement of an RBD polypeptide turn with the amino acid sequence of -H_{344}-E-N-R-P-G_{349}-. Histidine-344 and asparagine-346 interact with the serine effector in the inhibited enzyme, demonstrating that the observed conformational change may be initiated with serine binding (*5*).

Aside from the 344−349 loop movement, the coordinate overlays described in the Results section suggest that the RBD−SBD domains and NBD domain in the two forms of the enzyme are virtually superimposable when done independently. The conformational changes observed between the RBD−SBD and NBD must then involve the linkage between the two. As noted above, this linkage involves two segments of polypeptide chain that together permit a hinge or turning motion. By analyzing the crystallographic coordinate sets using the principles and computer program of Hayward et al. (*22*, *26*), the entire conformational change could be described by a relatively simple rotation around an arbitrary axis. The crossovers between domains have alternately been labeled hinge.

To further define residues capable of relaying conformational change, a comparison of the ϕ,ψ angles through the linkages was carried out by averaging the four copies of coordinates for the serine-free enzyme (contents of one crystallographic asymmetric unit) and the two copies of the serine-inhibited enzyme. As noted in the Results section, torsional angle changes appear to involve residues -P_{105}-F-S-N_{108}- and -I_{293}-G-G_{295}-. Both strands of the SBD to NBD link or hinge are close to the nicotinamide ring of the bound coenzyme. In fact, the amide nitrogen of G_{294} is hydrogen bonded to the carboxyamide of the bound coenzyme so that a linkage in the crystal structures is established between the allosteric regulation and the catalytic activity. A major main-chain torsional change of 180° is also noted for I293 within the hinge and immediately adjacent to the catalytic histidine. Therefore, continuity between the serine binding site(s) and the active site is clearly established via the two-membered crossover between RBD−SBD and NBD.

Finally, with respect to other enzymes that contain the ACT domain, one may speculate that their allosteric control mechanism may function similarly. Binding of effector would take place at the ends of β-strands at a subunit interface, interacting with ligands from both subunits. This would result in a conformational change that is linked to a second and possibly third domain involved in catalysis. This could represent a general mechanism among an entire group of enzymes that contain ACT domains. In PGDH from *E. coli*, it appears that substrate binds to an open active site cleft and is brought into proximity of the catalytic residues as the cleft closes. This appears to be the basis for the V_{max}-type regulation observed with PGDH, with the effector inhibiting cleft closing rather than substrate binding. Further study will reveal whether V_{max}-type regulation will continue to be a property of all ACT domain-containing proteins or if it will extend to K_m-type inhibition systems as well.

ACKNOWLEDGMENT

We especially acknowledge the continuing help of Ed Hoeffner, who maintains our X-ray diffraction, light scattering, and calorimetry resources. The Mass Spectrometry Facility at the University of Minnesota provided the instrumentation and expertise for this ES-MS work. We are grateful to the Minnesota Supercomputer Institute for computational resources especially the continuing use of the Biomedical Sciences Computing Laboratory under the direction of Dr. Patton Fast.

REFERENCES

1. Slaughter, J. C., and Davies, D. D. (1968) Inhibition of 3-phosphoglycerate dehydrogenase by L-serine, *Biochem. J. 109*, 749−555.
2. Dubrow, R., and Pizer, L. (1977) Transient kinetic and deuterium isotope effect studies on the catalytic mechanism of phosphoglycerate dehydrogenase, *J. Biol. Chem. 252*, 1539−1551.
3. Grant, G. (1989) A new family of 2-hydroxyacid dehydrogenases, *Biochem. Biophy. Res. Commun. 165*, 1371−1374.
4. Grant, G., Hu, Z., and Lan Xu, X. (2001) Amino acid residue mutations uncouple cooperative effects in *Escherichia coli* D-3-phonphoglycerate dehydrogenase, *J. Biol. Chem. 276*, 17844−17850.
5. Schuller, D. J., Grant, G. A., and Banaszak, L. J. (1995) The allosteric ligand site in the V_{max}-type cooperative enzyme phosphoglycerate dehydrogenase, *Nat. Struct. Biol. 2*, 69−75.
6. Al-Rabiee, R., Lee, A. J., and Grant, G. A. (1996) The mechanism of velocity modulated allosteric regulation in D-3-phosphoglycerate dehydrogenase: Cross-linking adjacent regulatory domains with engineered disulfides mimics effector binding, *J. Biol. Chem. 271*, 13013−13017.
7. Bell, J., Bell, E., Pease, P., Grant, G., and Banaszak, L. (2002) De-regulation of D-3-phosphoglycerate dehydrogenase by domain removal, *Eur. J. Biochem. 269*, 1−9.
8. Lamzin, V. S., Dauter, Z., Popov, V. O., Harutyunyan, E. H., and Wilson, K. S. (1994) High-resolution structures of holo and apo formate dehydrogenase, *J. Mol. Biol. 236*, 759−785.
9. Grant, G. A., Schuller, D. J., and Banaszak, L. J. (1996) A Model for the regulation of D-3-phosphoglycerate dehydrogenase, a V_{max}-type allosteric enzyme, *Protein Sci. 5*, 34−41.
10. Bell, J. K., Grant, G. A., and Banaszak, L. J. (2004) Multiconformational states in phosphoglycerate dehydrogenase, *Biochemistry 43*, 3450−3458.
11. Grant, H., and Xu, L. (2001) Specific interactions at the regulatory domain-substrate binding domain interface influence the cooperativity of inhibition and effector binding in *Escherichia coli* D-3-phosphoglycetrate dehydrogenase, *J. Biol. Chem. 276*, 1078−1083.
12. Aravind, L., and Koonin, E. (1999) Gleaning non-trivial structural, functional and evolutionary information about protein by iterative database searches, *J. Mol. Biol. 287*, 1023−1040.
13. Chipman, D. M., and Shaanan, B. (2001) The ACT domain family, *Curr. Opin. Chem. Biol. 11*, 694−700.
14. Zhao, G., and Winkler, M. E. (1996) A novel alpha-ketoglutarate reductase activity of the serA-encoded 3-phosphoglycerate dehydrogenase of *Escherichia coli* K-12 and its possible implications for human 2-hydroxyglutaric aciduria, *J. Bacteriol. 178*, 232−239.
15. Tobey, K. L., and Grant, G. A. (1986) The nucleotide sequence of the sera gene of *Escherichia coli* and the amino acid sequence of the encoded protein, D-3-phosphoglycerate dehydrogenase, *J. Biol. Chem. 261*, 12179−12183.
16. Schuller, D. J., Fetter, C. H., Banaszak, L. J., and Grant, G. A. (1989) Enhanced expression of the *Escherichia coli serA* gene in a plasmid vector. Purification, crystallization, and preliminary X-ray data of D-3-phosphoglycerate dehydrogenase, *J. Biol. Chem. 264*, 2645−2648.
17. Novagen (2003) Enhanced Protein Coexpression in *E. coli*, Madison, WI.
18. Golden, B., Hoffman, D., Ramakrishnan, V., and White, S. (1993) Ribosomal protein-S17−Characterization of the 3-dimensional structure by H-1-NMR and N-15-NMR, *Biochemistry 32*, 12812−12820.
19. Terwilliger, T. C. (2002) Rapid automatic NCS identification using heavy-atom substructures, *Acta Crystallogr., Sect. D 58*, 2213−2215.
20. Brunger, A. T., Adams, P. D., Clore, G. M., Delano, W. L., Gros, P., Grossekunstleve, R. W., Jiang, J. S., Kuszewski, J., Nilges, M., Pannu, N. S., Read, R. J., Rice, L. M., Simonson, T., and Warren, G. L. (1998) Crystallography and NMR system−A new software suite for macromolecular structure determination, *Acta Crystallogr., Sect. D 54*, 905−921.
21. Perrakis, A. (2001) ARP/wARP and molecular replacement, *Acta Crystallogr., Sect. D 57*, 1445−1450.
22. Hayward, S., Kitao, A., and Berendsen, H. J. C. (1997) Model-free methods of analyzing domain motions in proteins from simulation: A comparison of normal mode analysis and molecular dynamics simulation of lysozyme, *Proteins 27*, 425−437.

23. Hayward, S., and Berendsen, H. J. C. (1998) Systematic analysis of domain motions in proteins from conformational change—New results on citrate synthase and T4 lysozyme, *Proteins 30*, 144−154.
24. DeLano, W. L. (2002) The PyMOL Molecular Graphics System, World Wide Web http://www.pymol.org.
25. Laskowski, R., MacArthur, M., Moss, D., and Thornton, J. M. (1993) Procheck—A program to check the stereochemical quality of protein structures, *J. Appl. Crystallogr. 26*, 283−291.
26. Hayward, S. (1999) Structural principles governing domain motions in proteins, *Proteins 36*, 425−435.
27. Grant, G. A., Kim, S. J., Xu, X. L., and Hu, Z. (1999) The contribution of adjacent subunits to the active sites of D-3-phosphoglycerate dehydrogenase, *J. Biol. Chem. 274*, 5357−5361.
28. Grant, G. A., Xu, X. L., Hu, Z., and Purvis, A. R. (1999) Phosphate ion partially relieves the cooperativity of effector binding in D-3-phosphoglycerate dehydrogenase without altering the cooperativity of inhibition, *Biochemistry 38*, 16548−16552.
29. Christopher, J. A. (1988) in *SPOCK, The Structural Properties Observation and Calculation Kit*, Center for Macromolecular Design, Texas A&M University, College Station, TX.
30. Jones, T. A., Zou, J. Y., Cowan, S. W., and Kjeldgaard, M. (1991) Improved methods for building protein models in electron density maps and the location of errors in these models, *Acta Crystallogr. A47*, 110−119.
31. Rodriguez, R., Chinea, G., Lopez, N., Pons, T., and Vriend, G. (1998) Homology modeling, model and software evaluation: three related resources, *Bioinformatics 14*, 523−528.

BI047944B